Design and Characterization of Permanent Magnetic Solenoids for REGAE

2nd EAAC Workshop - WG4

Max Hachmann

DESY

Elba, September 14, 2015

Outline

Outline

Motivation

Design

Assembling

Simulations

Field measurements

Conclusions

REGAE

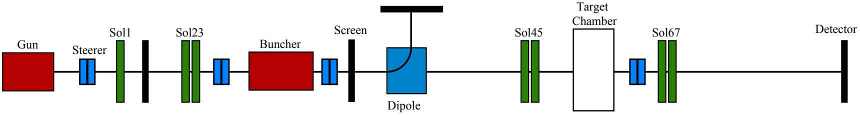

total length	9.5 m
$\mathbf{E_{kin}}$	5 MeV
$\Delta \mathbf{p_z}$	$\sim$ 10 keV/c
bunch length	$\sim$ 10 fs $\hat{=}$ 3 μm
bunch charge	< 100 fC $(< 0.5 \cdot 10^6\ e^-)$
trans. norm. emittance	$\sim 0.01\,\pi$ mm mrad

LAOLA@REGAE[1]

Laser parameter		Bunch parameter	
Laser pulse energy	5 J	E_{kin}	7 MeV–13 MeV
Laser pulse length	25 fs–100 fs	Δp_z	$\sim$ 200 kev/c
Laser focus spot size	40 µm	**norm. emittance**	???
Plasma density	$10^{16}\,\mathrm{cm}^{-3}$		

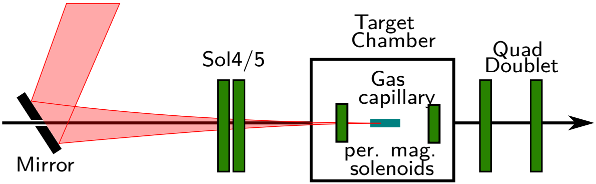

Figure 1: Setup for external injection in a laser-plasma wakefield

[1] B. Zeitler et al., "Merging conventional and laser wakefield accelerators", in *Proc. SPIE*, vol. 8779, 2013.

Permanent magnetic Solenoids

Requirements:

- strong focusing $\rightarrow \sim 2\,\mu m$@injection point

Permanent magnetic Solenoids

Requirements:

- strong focusing $\rightarrow \sim 2\,\mu m$@injection point
- close to injection point

Permanent magnetic Solenoids

Requirements:

- strong focusing $\rightarrow \sim 2\,\mu\text{m}$@injection point
- close to injection point

Solution:

Permanent magnetic Solenoids

Requirements:

- strong focusing $\rightarrow \sim 2\,\mu\text{m}$@injection point
- close to injection point

Solution:

- In-vacuum solution:
  - permanent magnetic material (NdFeB)
  - high surface current density
  - strong focusing

Permanent magnetic Solenoids

Requirements:

- strong focusing $\rightarrow \sim 2\,\mu\mathrm{m}$@injection point
- close to injection point

Solution:

- In-vacuum solution:
  - permanent magnetic material (NdFeB)
  - high surface current density
  - strong focusing

Permanent magnetic Solenoids

Requirements:

> strong focusing $\rightarrow \sim 2\,\mu m$@injection point

> close to injection point

Solution:

> In-vacuum solution:

- permanent magnetic material (NdFeB)
- high surface current density
- strong focusing

> focusing in both trans. directions

Permanent magnetic Solenoids

Requirements:

- strong focusing $\rightarrow \sim 2\,\mu\text{m}$@injection point
- close to injection point

Solution:

- In-vacuum solution:
  - permanent magnetic material (NdFeB)
  - high surface current density
  - strong focusing
- focusing in both trans. directions
- In-vacuum movers for alignment and focus adjustment

Outline

Design and mag. field[2]

- design is optimized in terms of:
  - focusing strength
  - emittance growth
  - weight (<1.5 kg)

[2] T. Gehrke, "Design of permanent magnetic solenoids for REGAE", Master's thesis, University of Hamburg, Germany, 2013.

Design and mag. field[2]

- design is optimized in terms of:
  - focusing strength
  - emittance growth
  - weight (<1.5 kg)
- two ring design

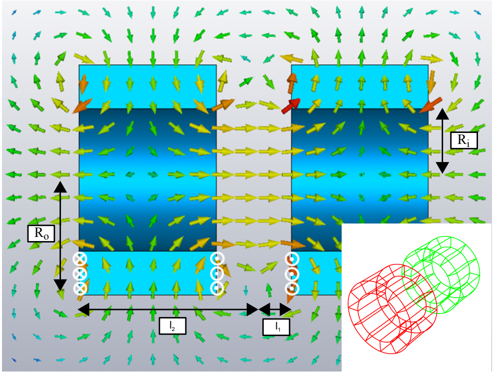

Figure 2: CST simulation and wedge arrangement.

[2] T. Gehrke, "Design of permanent magnetic solenoids for REGAE", Master's thesis, University of Hamburg, Germany, 2013.

Design and mag. field[2]

- design is optimized in terms of:
  - focusing strength
  - emittance growth
  - weight (<1.5 kg)
- two ring design
- each ring is made of 12 wedges

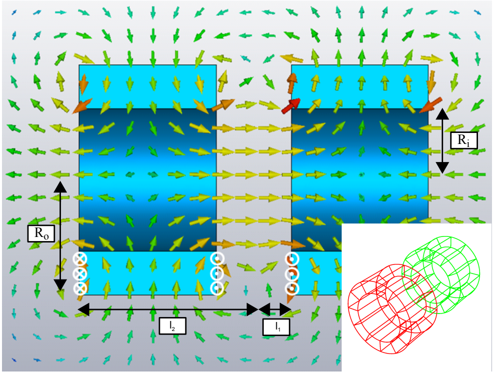

Figure 2: CST simulation and wedge arrangement.

[2]T. Gehrke, "Design of permanent magnetic solenoids for REGAE", Master's thesis, University of Hamburg, Germany, 2013.

Design and mag. field[2]

- design is optimized in terms of:
  - focusing strength
  - emittance growth
  - weight (<1.5 kg)
- two ring design
- each ring is made of 12 wedges
- wedges are radially magnetized

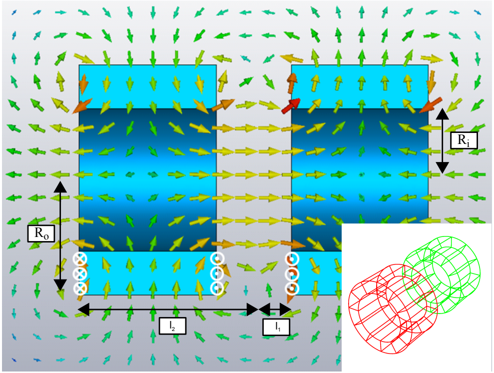

Figure 2: CST simulation and wedge arrangement.

[2] T. Gehrke, "Design of permanent magnetic solenoids for REGAE", Master's thesis, University of Hamburg, Germany, 2013.

Design and mag. field[2]

- design is optimized in terms of:
  - focusing strength
  - emittance growth
  - weight (<1.5 kg)
- two ring design
- each ring is made of 12 wedges
- wedges are radially magnetized

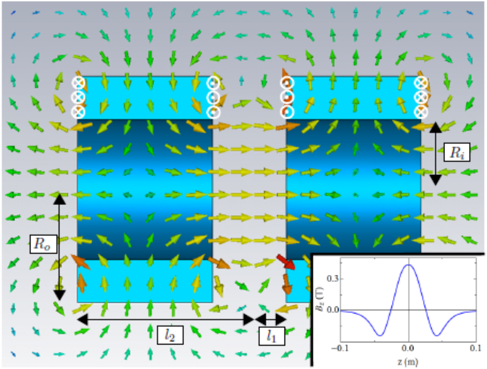

Figure 2: CST simulation and long. on-axis field B_z.

[2] T. Gehrke, "Design of permanent magnetic solenoids for REGAE", Master's thesis, University of Hamburg, Germany, 2013.

LAOLA.

Design and mag. field[2]

R_i [mm]	17
R_o [mm]	25.4
l_1 [mm]	7.8
l_2 [mm]	44.8
m [kg]	0.625
$B_{z,max}$ [T]	~ 0.44
f@5 MeV [m]	~ 0.18

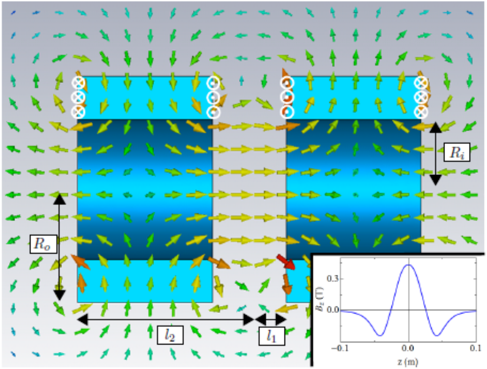

Figure 2: CST simulation and long. on-axis field B_z.

[2] T. Gehrke, "Design of permanent magnetic solenoids for REGAE", Master's thesis, University of Hamburg, Germany, 2013.

LAOLA.

Outline

Motivation

Design

Assembling

Simulations

Field measurements

Conclusions

Necessity of sorting algorithm

- Flawed wedges reduce field quality

Necessity of sorting algorithm

- Flawed wedges reduce field quality
- Magnetization errors cancel out for the right permutation

Necessity of sorting algorithm

- Flawed wedges reduce field quality
- Magnetization errors cancel out for the right permutation
- Two rings consist of 24 wedges
- $12! \cdot 12! \sim 2 \cdot 10^{17}$ permutations

Necessity of sorting algorithm

- Flawed wedges reduce field quality
- Magnetization errors cancel out for the right permutation
- Two rings consist of 24 wedges
- $12! \cdot 12! \sim 2 \cdot 10^{17}$ permutations
- pool of ~ 100 wedges

Necessity of sorting algorithm

- Flawed wedges reduce field quality
- Magnetization errors cancel out for the right permutation
- Two rings consist of 24 wedges
- $12! \cdot 12! \sim 2 \cdot 10^{17}$ permutations
- pool of ~ 100 wedges
- fast and 'intelligent' sorting algorithm required
  - analytical field description
  - quantity for field quality in order to optimize

Analytical field description

- Describing mag. field via rectangular wire loops by means of *Biot-Savart's law*
- Orientation errors can be described by tilt of loops
- Magnetization strength error can be corrected via wire loop current

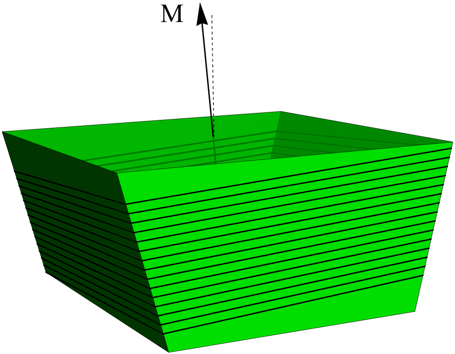

$$\mathbf{B}(\mathbf{r}) = \sum_{i=1}^{N} \sum_{j=1}^{4} \left(\frac{\mu_0}{4\,\pi} \int_{l_{ij}} \mathbf{I}(\mathbf{r}') \times \frac{\mathbf{r}-\mathbf{r}'}{|\mathbf{r}-\mathbf{r}'|^3} \, \mathrm{d}l \right)$$

Field goodness

- Aim: small emittance growth

Field goodness

- Aim: small emittance growth
- Criterion: 4D-emittance-like quantity

Field goodness

- Aim: small emittance growth
- Criterion: 4D-emittance-like quantity

$$\epsilon_{\mathrm{4D}}^2 \sim \begin{vmatrix} \langle x^2\rangle & \langle xp_x\rangle & \langle xy\rangle & \langle xp_y\rangle \\ \langle xp_x\rangle & \langle p_x^2\rangle & \langle yp_x\rangle & \langle p_x p_y\rangle \\ \langle xy\rangle & \langle yp_x\rangle & \langle y^2\rangle & \langle yp_y\rangle \\ \langle xp_y\rangle & \langle p_x p_y\rangle & \langle yp_y\rangle & \langle p_y^2\rangle \end{vmatrix}$$

Field goodness

- Aim: small emittance growth
- Criterion: 4D-emittance-like quantity

$$\epsilon_{4\mathrm{D}}^2 \sim \begin{vmatrix} \langle x^2 \rangle & \langle xp_x \rangle & \langle xy \rangle & \langle xp_y \rangle \\ \langle xp_x \rangle & \langle p_x^2 \rangle & \langle yp_x \rangle & \langle p_x p_y \rangle \\ \langle xy \rangle & \langle yp_x \rangle & \langle y^2 \rangle & \langle yp_y \rangle \\ \langle xp_y \rangle & \langle p_x p_y \rangle & \langle yp_y \rangle & \langle p_y^2 \rangle \end{vmatrix}$$

- Assumptions for 'particle tracking':

Field goodness

- Aim: small emittance growth
- Criterion: 4D-emittance-like quantity

$$\epsilon_{4\mathrm{D}}^2 \sim \begin{vmatrix} \langle x^2 \rangle & \langle x p_x \rangle & \langle xy \rangle & \langle x p_y \rangle \\ \langle x p_x \rangle & \langle p_x^2 \rangle & \langle y p_x \rangle & \langle p_x p_y \rangle \\ \langle xy \rangle & \langle y p_x \rangle & \langle y^2 \rangle & \langle y p_y \rangle \\ \langle x p_y \rangle & \langle p_x p_y \rangle & \langle y p_y \rangle & \langle p_y^2 \rangle \end{vmatrix}$$

- Assumptions for 'particle tracking':
  1. zero emittance; ring-like distribution

Field goodness

- Aim: small emittance growth
- Criterion: 4D-emittance-like quantity

$$\epsilon_{4\mathrm{D}}^2 \sim \begin{vmatrix} \langle x^2 \rangle & \langle x p_x \rangle & \langle xy \rangle & \langle x p_y \rangle \\ \langle x p_x \rangle & \langle p_x^2 \rangle & \langle y p_x \rangle & \langle p_x p_y \rangle \\ \langle xy \rangle & \langle y p_x \rangle & \langle y^2 \rangle & \langle y p_y \rangle \\ \langle x p_y \rangle & \langle p_x p_y \rangle & \langle y p_y \rangle & \langle p_y^2 \rangle \end{vmatrix}$$

- Assumptions for 'particle tracking':
  1. zero emittance; ring-like distribution
  2. 'infinitive' high energy $\rightarrow$ beam size constant

Field goodness

- Aim: small emittance growth
- Criterion: 4D-emittance-like quantity

$$\epsilon_{4\mathrm{D}}^2 \sim \begin{vmatrix} \langle x^2 \rangle & \langle x p_x \rangle & \langle xy \rangle & \langle x p_y \rangle \\ \langle x p_x \rangle & \langle p_x^2 \rangle & \langle y p_x \rangle & \langle p_x p_y \rangle \\ \langle xy \rangle & \langle y p_x \rangle & \langle y^2 \rangle & \langle y p_y \rangle \\ \langle x p_y \rangle & \langle p_x p_y \rangle & \langle y p_y \rangle & \langle p_y^2 \rangle \end{vmatrix}$$

- Assumptions for 'particle tracking':
  1. zero emittance; ring-like distribution
  2. 'infinitive' high energy $\rightarrow$ beam size constant
  3. 'particles' move on a straight line

Field goodness

- Aim: small emittance growth
- Criterion: 4D-emittance-like quantity

$$\epsilon_{4\mathrm{D}}^2 \sim \begin{vmatrix} \langle x^2 \rangle & \langle x p_x \rangle & \langle xy \rangle & \langle x p_y \rangle \\ \langle x p_x \rangle & \langle p_x^2 \rangle & \langle y p_x \rangle & \langle p_x p_y \rangle \\ \langle xy \rangle & \langle y p_x \rangle & \langle y^2 \rangle & \langle y p_y \rangle \\ \langle x p_y \rangle & \langle p_x p_y \rangle & \langle y p_y \rangle & \langle p_y^2 \rangle \end{vmatrix}$$

- Assumptions for 'particle tracking':
  1. zero emittance; ring-like distribution
  2. 'infinitive' high energy $\rightarrow$ beam size constant
  3. 'particles' move on a straight line
  4. Lorentz force:
     - $p_x \sim -\int_a^b B_y \,\mathrm{d}z$
     - $p_y \sim \int_a^b B_x \,\mathrm{d}z$

Field Goodness

In front of PMS:

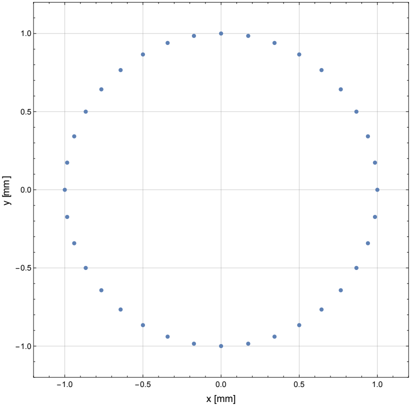

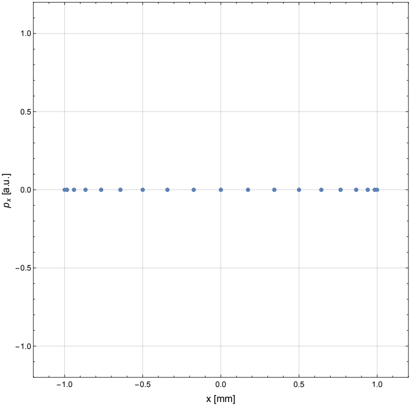

Field Goodness

Behind PMS:

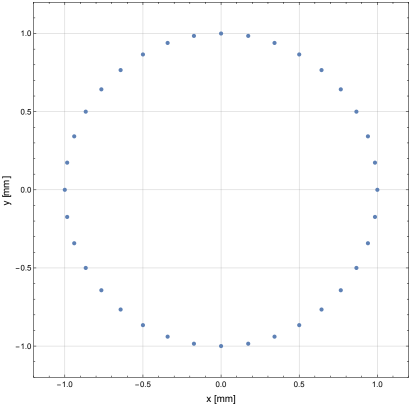

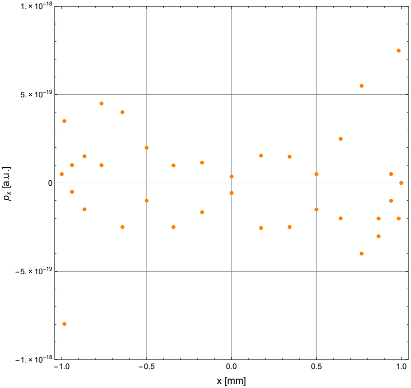

Field Goodness

Behind PMS:

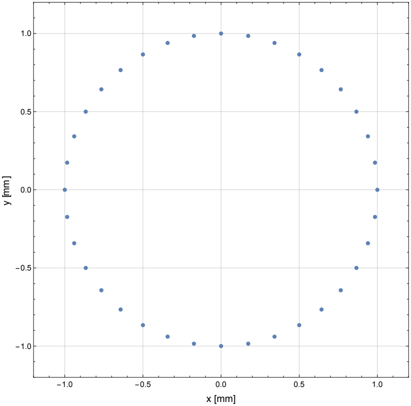

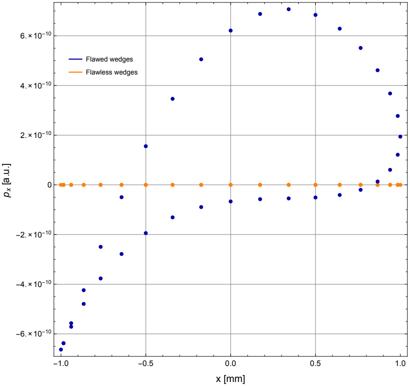

1^{st} level Sorting: Random Arrangement

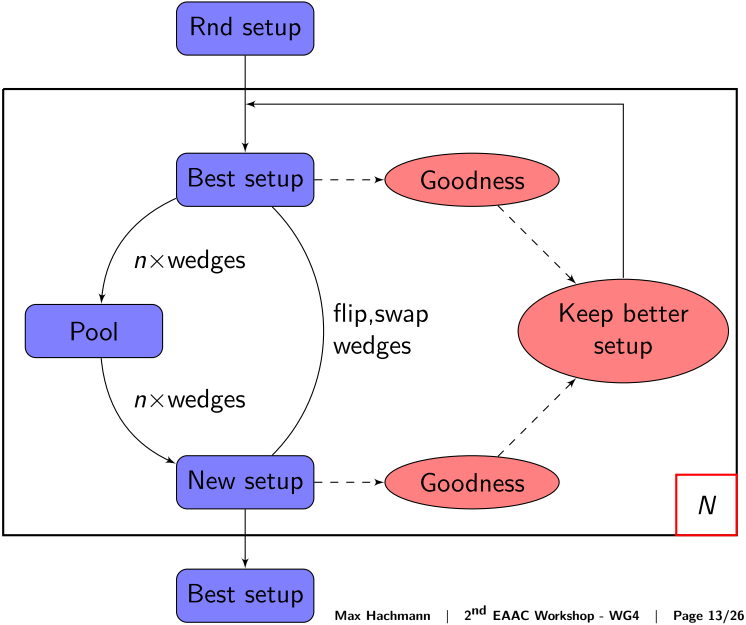

2^{nd} level Sorting: simulated annealing[3]

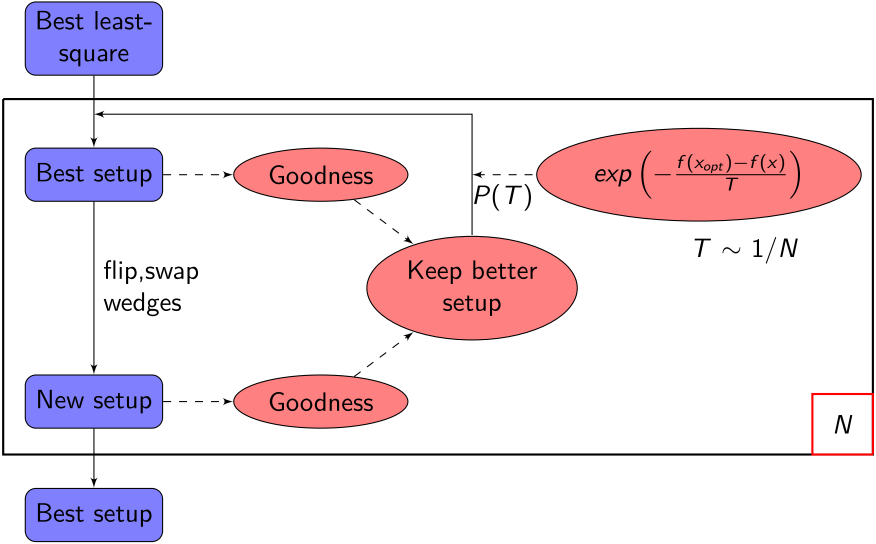

[3]S. Kirkpatrick et al., "Optimization by simulated annealing", *Science*, vol. 220, no. 4598, pp. 671–680, 1983.

Emittance growth

ASTRA simulation

- $\epsilon_x = \epsilon_y = 0$
- $x_{RMS} = y_{RMS} = 610\,\mu m$
- no space-charge
- $E_{kin} = 5\,\mathrm{MeV}$

Emittance growth

ASTRA simulation

- $\epsilon_x = \epsilon_y = 0$
- $x_{RMS} = y_{RMS} = 610\,\mu\text{m}$
- no space-charge
- $E_{kin} = 5\,\text{MeV}$

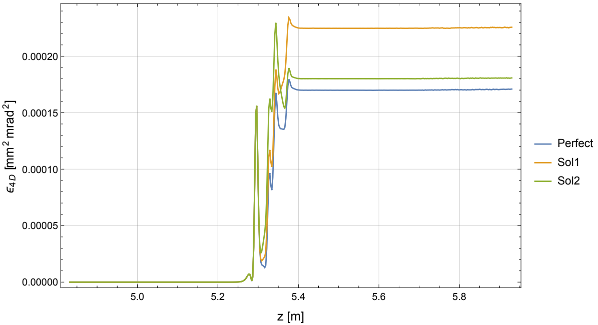

	Sol1	Sol2
$\epsilon_{\text{flawed}} / \epsilon_{\text{flawless}}$	1.32	1.06

Emittance growth

ASTRA simulation

- $\epsilon_x = \epsilon_y = 0$
- $x_{RMS} = y_{RMS} = 610\,\mu m$
- no space-charge
- $E_{kin} = 5\,\text{MeV}$

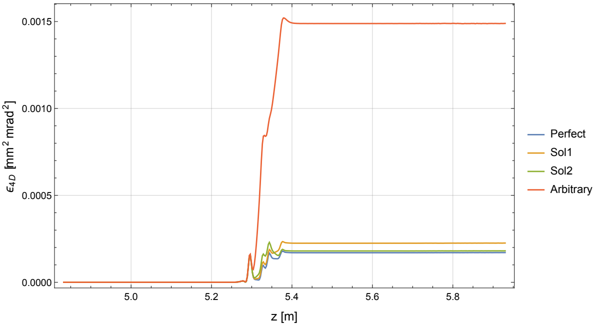

	Sol1	Sol2	arbitrary
$\epsilon_{\text{flawed}}/\epsilon_{\text{flawless}}$	1.32	1.06	8.71

Proof of goodness criterion

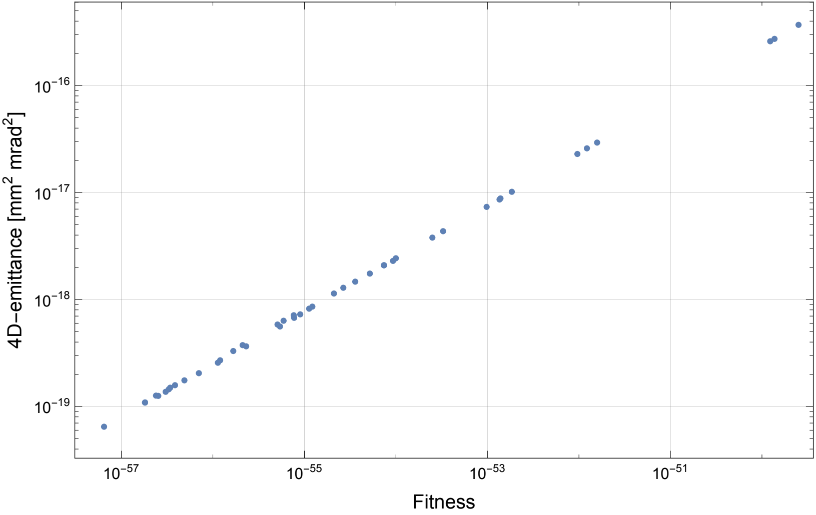

Outline

Beam focusing for external injection at REGAE

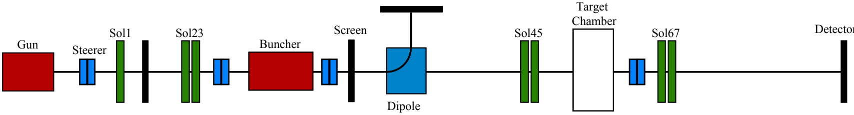

- $\epsilon_{n,x} = 0.041\,\text{mm mrad}$
- $x_{RMS} = y_{RMS} = 0.707\,\text{mm}$
- $Q = 100\,\text{fC}$
- $E_{kin} = 5.58\,\text{MeV}$

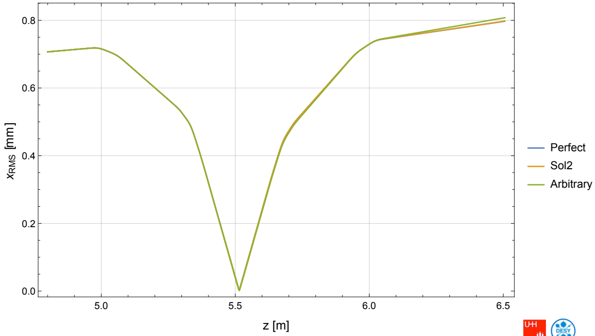

Beam focusing for external injection at REGAE

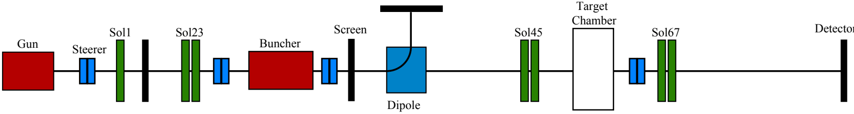

- $\epsilon_{n,x} =$ 0.041 mm mrad
- $x_{RMS} = y_{RMS} =$ 0.707 mm
- $Q = 100$ fC
- $E_{kin} = 5.58$ MeV

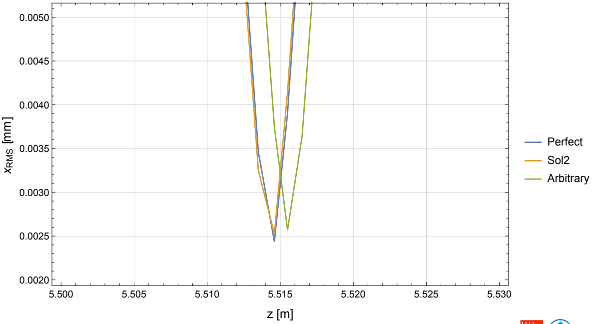

LAOLA.

Beam focusing for external injection at REGAE

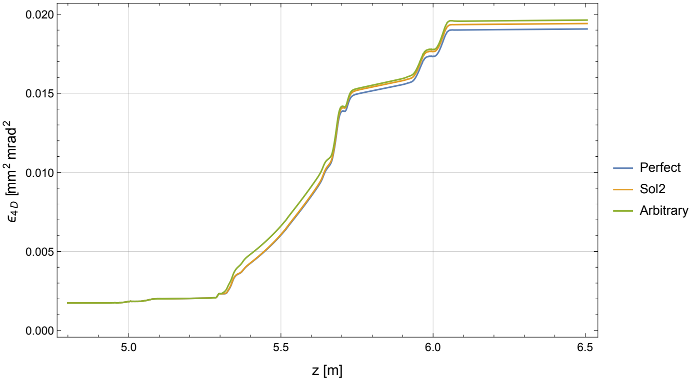

Beam focusing for external injection at REGAE

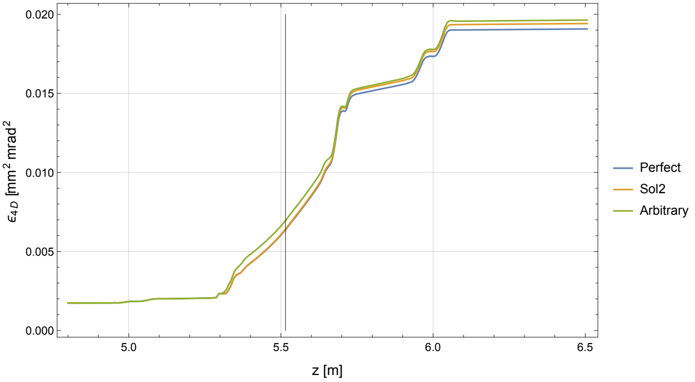

	Sol1	Arbitrary
$\epsilon_{\text{flawed}} / \epsilon_{\text{flawless}}$	1.01	1.10

Beam focusing for external injection at REGAE

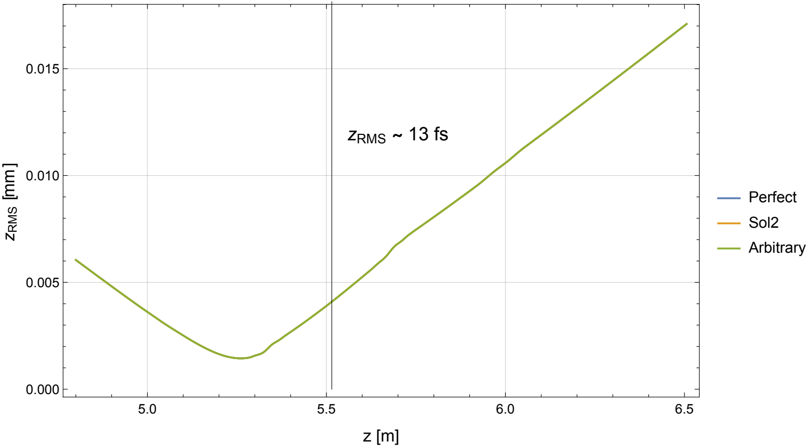

Outline

Motivation

Design

Assembling

Simulations

Field measurements

Conclusions

LAOLA.

Hall probe

Requirements:

- relative precision $\rightarrow \sim 10 \times 10^{-4}$ (earth's magnetic field)
- small active volume $\rightarrow$ high gradients; nonlinear
- small dimensions $\rightarrow \sim 35\,\text{mm}$ inner diameter

Hall probe

Requirements:

- relative precision $\rightarrow \sim 10 \times 10^{-4}$ (earth's magnetic field)
- small active volume $\rightarrow$ high gradients; nonlinear
- small dimensions $\rightarrow \sim 35\,\text{mm}$ inner diameter

Hall probe:

- Metrolab THM1176-HF
- 3-axes Hall probe
- active volume: $(150 \times 150 \times 10)\,\mu\text{m}^3$

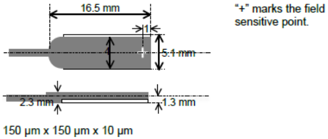

Metrolab 3D-Hall probe: Calibration

> Calibration relative to Metrolab-NMR probe of MEA in a dipole magnet

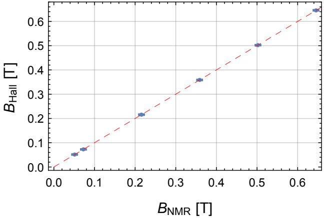

slope	0.999 98(9)
offset	$1.08(3) \times 10^{-4}$

Metrolab 3D-Hall probe: Calibration

- Calibration relative to Metrolab-NMR probe of MEA in a dipole magnet

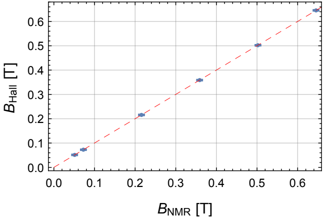

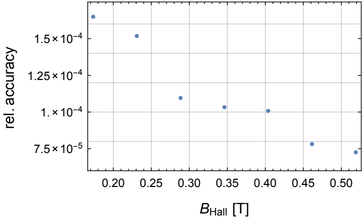

slope	$0.999\,98(9)$
offset	$1.08(3) \times 10^{-4}$

Measured and simulated field

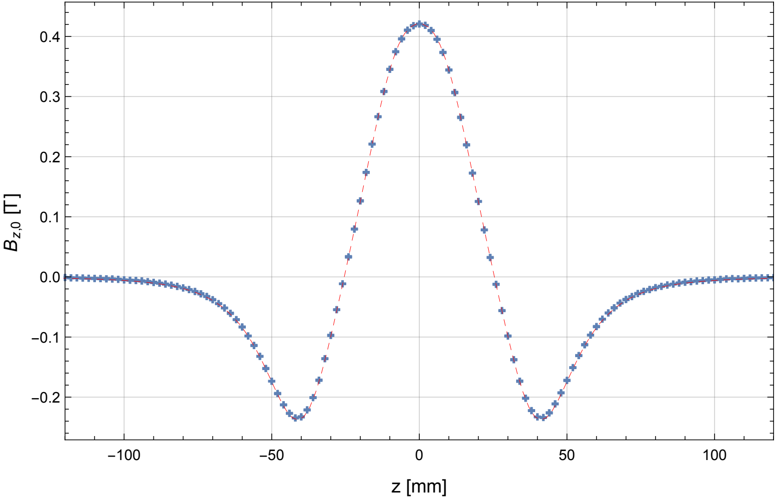

Figure 3: Long. field profile - measured and simulated.

LAOLA.

Measured and simulated field

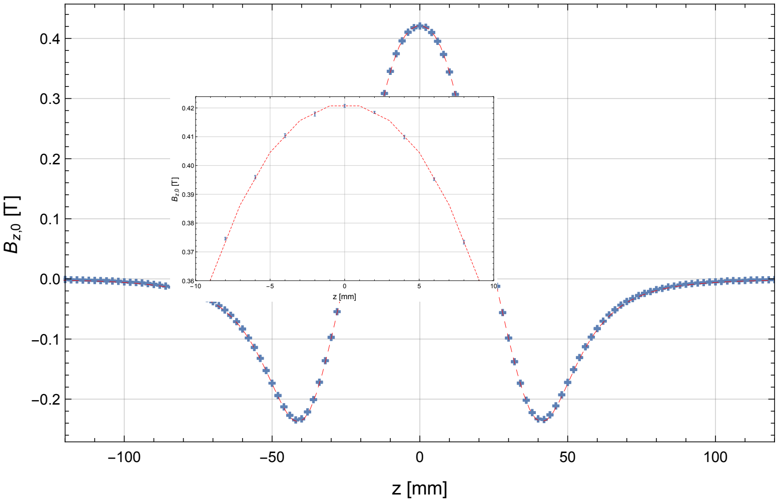

Figure 3: Long. field profile - measured and simulated.

Measured and simulated field

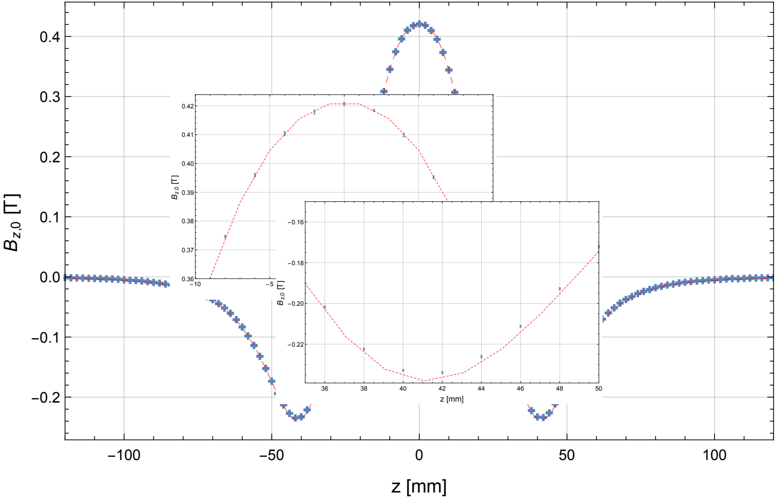

Figure 3: Long. field profile - measured and simulated.

Measured and simulated field

	$\mathbf{B_{z,max}}$ [T]	f@5 MeV [m]
simulated	0.44	0.18
measured	0.42	0.20

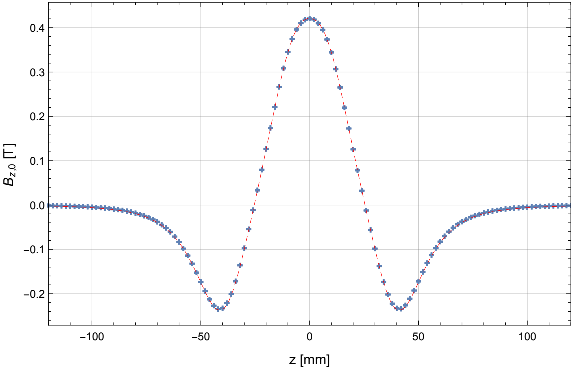

Figure 3: Long. field profile - measured and simulated.

Outline

LAOLA.

Conclusions/Outlook

- Successfully developed and assembled PMS
- Developed an analytical magnetic field simulation tool
  - Sorting algorithm
  - Magnetic field measurements (analytical simulation tool describes a real/measured solenoidal field)
- Beam-based measurements are lying ahead: alignment, focal beam size, emittance measurements, ...

Thank you for your attention.

Acknowledgment: F. Mayet, T. Gehrke, K. Floettmann, B. Zeitler

Bibliography

[1] T. Gehrke, "Design of permanent magnetic solenoids for REGAE", Master's thesis, University of Hamburg, Germany, 2013.

[2] S. Kirkpatrick, C. Gelatt, and M. P. Vecchi, "Optimization by simulated annealing", *Science*, vol. 220, no. 4598, pp. 671–680, 1983.

[3] B. Zeitler, I. Dornmair, T. Gehrke, M. Titberidze, A. R. Maier, B. Hidding, K. Floettmann, and F. Gruener, "Merging conventional and laser wakefield accelerators", in *Proc. SPIE*, vol. 8779, 2013.

LAOLA.

Benchmark: Number of current loops

> Reducing number of wire loops $\rightarrow$ speed-up calculations

Benchmark: Number of current loops

> Reducing number of wire loops → speed-up calculations

$$1/f \sim \int_{-\infty}^{\infty} {B_{z,0}}^2(z)\,\mathrm{d}z$$

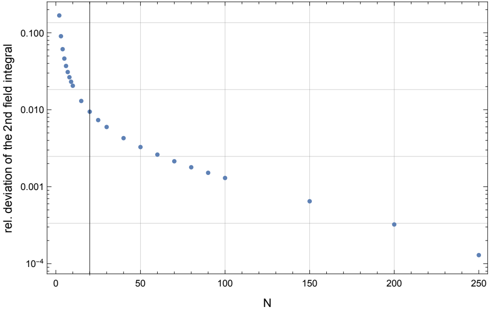

Benchmark: Number of current loops

> Reducing number of wire loops $\rightarrow$ speed-up calculations

$$1/f \sim \int_{-\infty}^{\infty} {B_{z,0}}^2(z)\,\mathrm{d}z$$

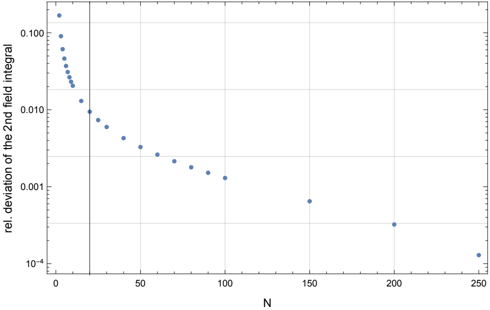

> $N = 20 \rightarrow 1\,\%$ accuracy

Benchmark: Convergence of Field Goodness

Benchmark: Convergence of Field Goodness

Number field lines:

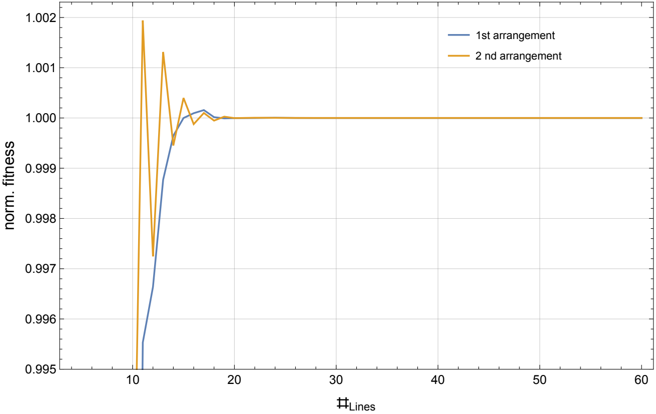

- $N_{\text{lines}} = 24$

Benchmark: Convergence of Field Goodness

Number of points along a line:

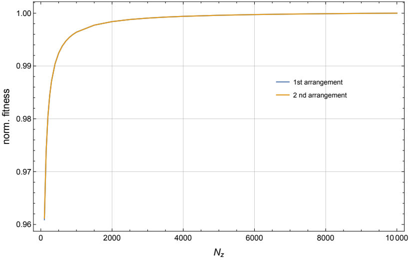

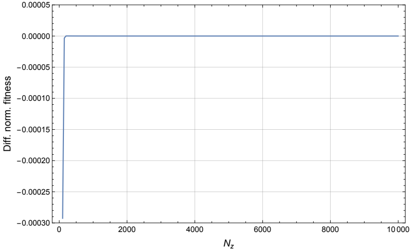

> $N_z = 500$

Background

$$\boldsymbol{B}_{back} = \begin{pmatrix} 0.0012 \\ -0.0014 \\ -0.0016 \end{pmatrix} \pm \begin{pmatrix} 0.0001 \\ 0.0001 \\ 0.0001 \end{pmatrix}$$

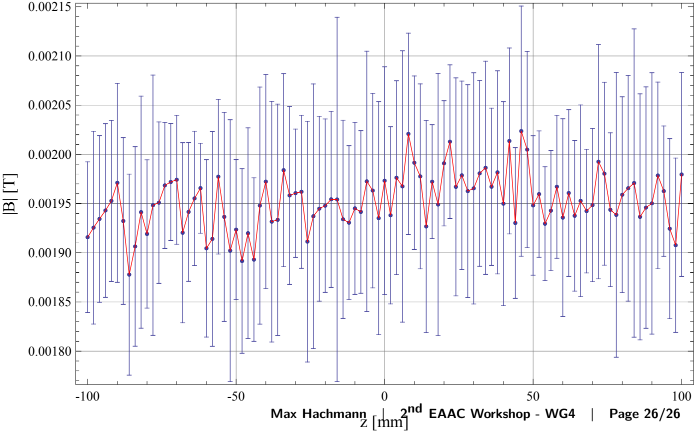

MEA1: Test stand

Stage:

- 3D linear stage
- smallest step: 12.5 μm
- hall probe fixed on a half profile brass lance

MEA1: Test stand

Stage:

- 3D linear stage
- smallest step: 12.5 µm
- hall probe fixed on a half profile brass lance

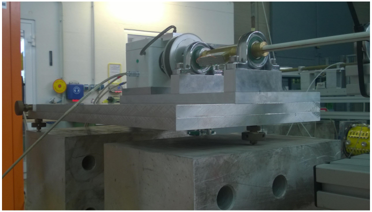

Adjustment table:

- 3 adjustable feet and 1 horizontal rotatable plate; manually
- min. step size: 12.5 µm

PMS alignment: Characteristic field properties

PMS alignment: Characteristic field properties

Polynomial series of a solenoidal field:

$$B_z(z,r) = B_{z,0} - \frac{r^2}{4}\frac{\mathrm{d}^2}{\mathrm{d}z^2}B_z(z) + \frac{r^4}{64}\frac{\mathrm{d}^4}{\mathrm{d}z^4}B_z(z)\ldots$$

$$B_r(z,r) = -\frac{r}{2}\frac{\mathrm{d}}{\mathrm{d}z}B_z(z) + \frac{r^3}{16}\frac{\mathrm{d}^3}{\mathrm{d}z^3}B_z(z) - \frac{r^5}{384}\frac{\mathrm{d}^5}{\mathrm{d}z^5}B_z(z)\ldots$$

PMS alignment: Characteristic field properties

Polynomial series of a solenoidal field:

$$B_z(z,r) = B_{z,0} - \frac{r^2}{4}\frac{\mathrm{d}^2}{\mathrm{d}z^2}B_z(z) + \frac{r^4}{64}\frac{\mathrm{d}^4}{\mathrm{d}z^4}B_z(z)\ldots$$

$$B_r(z,r) = -\frac{r}{2}\frac{\mathrm{d}}{\mathrm{d}z}B_z(z) + \frac{r^3}{16}\frac{\mathrm{d}^3}{\mathrm{d}z^3}B_z(z) - \frac{r^5}{384}\frac{\mathrm{d}^5}{\mathrm{d}z^5}B_z(z)\ldots$$

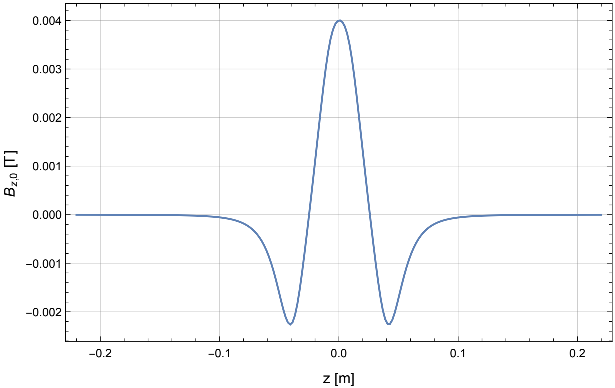

PMS alignment: Characteristic field properties

Polynomial series of a solenoidal field:

$$B_z(z,r) = B_{z,0} - \frac{r^2}{4}\frac{\mathrm{d}^2}{\mathrm{d}z^2}B_z(z) + \frac{r^4}{64}\frac{\mathrm{d}^4}{\mathrm{d}z^4}B_z(z)\ldots$$

$$B_r(z,r) = -\frac{r}{2}\frac{\mathrm{d}}{\mathrm{d}z}B_z(z) + \frac{r^3}{16}\frac{\mathrm{d}^3}{\mathrm{d}z^3}B_z(z) - \frac{r^5}{384}\frac{\mathrm{d}^5}{\mathrm{d}z^5}B_z(z)\ldots$$

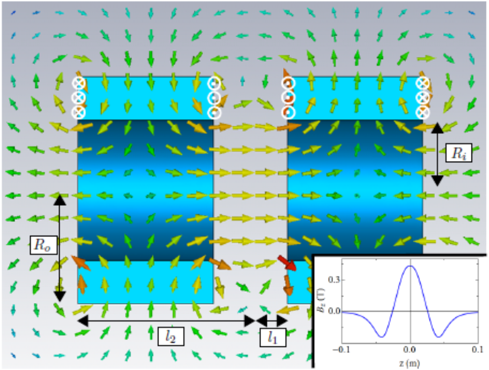

Prealignment and field measurements

- 9 degrees of freedom: $\{\underbrace{x,\ y,\ z}_{\text{Sol offset}},\ \underbrace{\alpha_x,\ \alpha_y,\ \alpha_z}_{\text{Sol tilt}},\ \underbrace{\beta_x,\ \beta_y,\ \beta_z}_{\text{Probe tilt}}\}$
- using zero field for PMS alignment

Prealignment and field measurements

- 9 degrees of freedom: $\{\underbrace{x,\, y,\, z}_{\text{Sol offset}},\, \underbrace{\alpha_x,\, \alpha_y,\, \alpha_z}_{\text{Sol tilt}},\, \underbrace{\beta_x,\, \beta_y,\, \beta_z}_{\text{Probe tilt}}\}$
- using zero field for PMS alignment
- probe is just aligned by eye

Prealignment and field measurements

- 9 degrees of freedom: $\{\underbrace{x,\, y,\, z}_{\text{Sol offset}},\, \underbrace{\alpha_x,\, \alpha_y,\, \alpha_z}_{\text{Sol tilt}},\, \underbrace{\beta_x,\, \beta_y,\, \beta_z}_{\text{Probe tilt}}\}$
- using zero field for PMS alignment
- probe is just aligned by eye
- measuring transversal plane at z_{Bmax} for probe alignment (post-processing)

Prealignment and field measurements

- 9 degrees of freedom: $\{\underbrace{x,\ y,\ z}_{\text{Sol offset}},\ \underbrace{\alpha_x,\ \alpha_y,\ \alpha_z}_{\text{Sol tilt}},\ \underbrace{\beta_x,\ \beta_y,\ \beta_z}_{\text{Probe tilt}}\}$
- using zero field for PMS alignment
- probe is just aligned by eye
- measuring transversal plane at z_{Bmax} for probe alignment (post-processing)

x-/y-probe-axes alignment

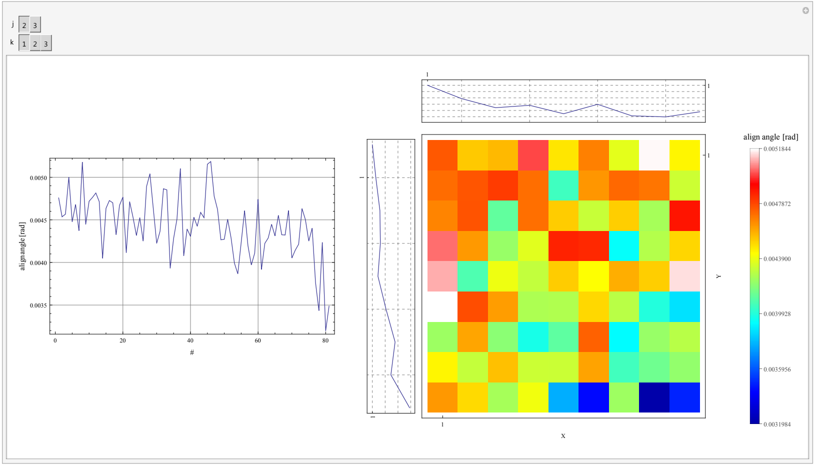

$$\beta_x = -0.007\,41(4)\ \text{rad} \qquad \beta_y = 0.004\,43(4)\ \text{rad}$$

Post-processing: Field fitting

remaining degrees of freedom: $\{x, y, z, \alpha_x, \alpha_y, \alpha_z, \beta_z\}$

Post-processing: Field fitting

remaining degrees of freedom: $\{x,\, y,\, z,\, \alpha_x,\, \alpha_y,\, \alpha_z,\, \beta_z\}$

Least-square-fit:

$$\chi^2 = \sum_i^N \left(\frac{|\boldsymbol{B}_{sim,i} - \boldsymbol{B}_{measure,i}|}{\sigma_i} \right)^2$$

> using simulated field for fitting

Post-processing: Field fitting

remaining degrees of freedom: $\{x, y, z, \alpha_x, \alpha_y, \alpha_z, \beta_z\}$

Least-square-fit:

$$\chi^2 = \sum_i^N \left(\frac{|\boldsymbol{B}_{sim,i} - \boldsymbol{B}_{measure,i}|}{\sigma_i} \right)^2$$

- using simulated field for fitting
- keeping the grid orientation but finer grid $\Rightarrow \{x, y, z\}$

Post-processing: Field fitting

remaining degrees of freedom: $\{x, y, z, \alpha_x, \alpha_y, \alpha_z, \beta_z\}$

Least-square-fit:

$$\chi^2 = \sum_i^N \left(\frac{|\boldsymbol{B}_{sim,i} - \boldsymbol{B}_{measure,i}|}{\sigma_i} \right)^2$$

- using simulated field for fitting
- keeping the grid orientation but finer grid $\Rightarrow \{x, y, z\}$
- rotating PMS in simulation $\Rightarrow \{\beta_x, \beta_y, \beta_z\}$

Post-processing: Field fitting

remaining degrees of freedom: $\{x, y, z, \alpha_x, \alpha_y, \alpha_z, \beta_z\}$

Least-square-fit:

$$\chi^2 = \sum_i^N \left(\frac{|\boldsymbol{B}_{sim,i} - \boldsymbol{B}_{measure,i}|}{\sigma_i} \right)^2$$

- using simulated field for fitting
- keeping the grid orientation but finer grid $\Rightarrow \{x, y, z\}$
- rotating PMS in simulation $\Rightarrow \{\beta_x, \beta_y, \beta_z\}$
- rotating simulated field around $\hat{e}_z \Rightarrow \alpha_z$

Post-processing: Field fitting

remaining degrees of freedom: $\{x, y, z, \alpha_x, \alpha_y, \alpha_z, \beta_z\}$

Least-square-fit:

$$\chi^2 = \sum_i^N \left(\frac{|\boldsymbol{B}_{sim,i} - \boldsymbol{B}_{measure,i}|}{\sigma_i} \right)^2$$

- using simulated field for fitting
- keeping the grid orientation but finer grid $\Rightarrow \{x, y, z\}$
- rotating PMS in simulation $\Rightarrow \{\beta_x, \beta_y, \beta_z\}$
- rotating simulated field around $\hat{e}_z \Rightarrow \alpha_z$
- offsets and α_z are not simulated; reduction of simulations

Post-processing: Field fitting

remaining degrees of freedom: $\{x,\, y,\, z,\, \alpha_x,\, \alpha_y,\, \alpha_z,\, \beta_z\}$

Least-square-fit:

$$\chi^2 = \sum_i^N \left(\frac{|\boldsymbol{B}_{sim,i} - \boldsymbol{B}_{measure,i}|}{\sigma_i} \right)^2$$

- using simulated field for fitting
- keeping the grid orientation but finer grid $\Rightarrow \{x,\, y,\, z\}$
- rotating PMS in simulation $\Rightarrow \{\beta_x,\, \beta_y,\, \beta_z\}$
- rotating simulated field around $\hat{e}_z \Rightarrow \alpha_z$
- offsets and α_z are not simulated; reduction of simulations

Field fitting routine

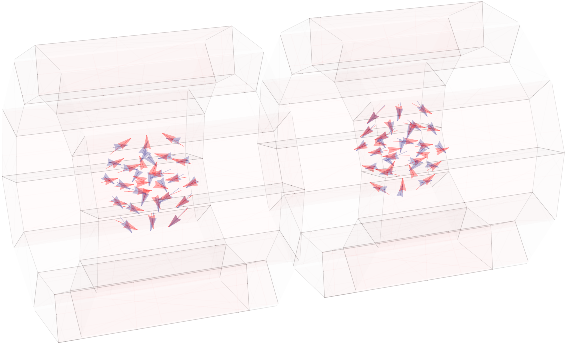

α_x [rad]	α_y [rad]	α_z [rad]	x [mm]	y [mm]	z [mm]	β_z [rad]
0	0	0	0	0	0	0

Field fitting routine

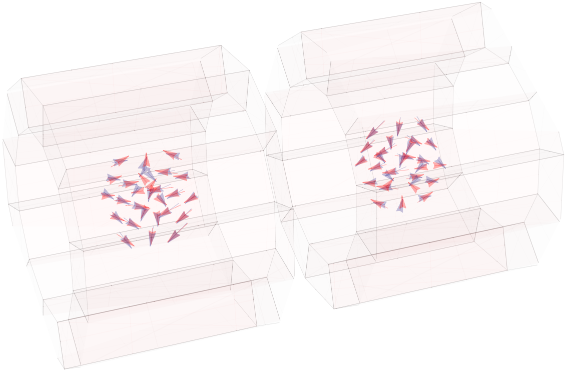

α_x [rad]	α_y [rad]	α_z [rad]	x [mm]	y [mm]	z [mm]	β_z [rad]
$\frac{\pi}{32}$	0	0	0	0	0	0

Field fitting routine

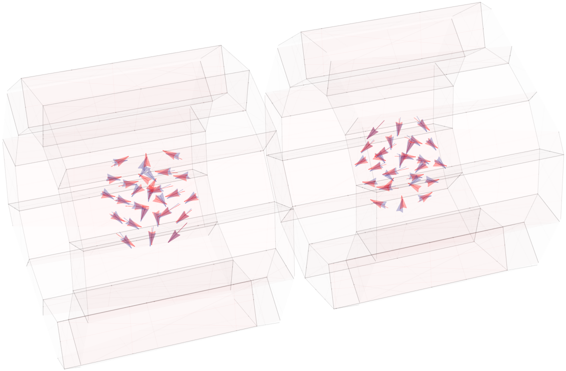

α_x [rad]	α_y [rad]	α_z [rad]	x [mm]	y [mm]	z [mm]	β_z [rad]
$\frac{\pi}{32}$	0	0	0	0	0	$\frac{\pi}{18}$

Field fitting routine

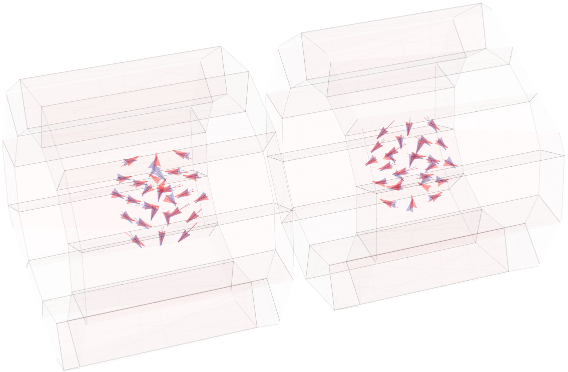

α_x [rad]	α_y [rad]	α_z [rad]	x [mm]	y [mm]	z [mm]	β_z [rad]
$\frac{\pi}{32}$	0	0	0	0	0.002	$\frac{\pi}{18}$

Field fitting routine

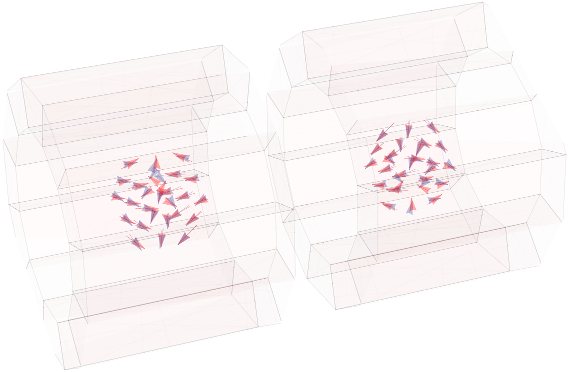

α_x [rad]	α_y [rad]	α_z [rad]	x [mm]	y [mm]	z [mm]	β_z [rad]
$\frac{\pi}{32}$	0	0	0	0.001	0.002	$\frac{\pi}{18}$

Field fitting routine

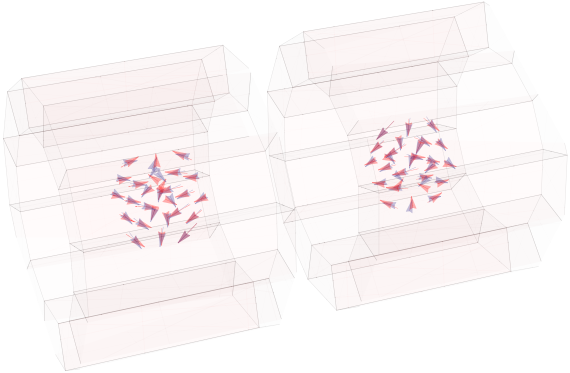

α_x [rad]	α_y [rad]	α_z [rad]	x [mm]	y [mm]	z [mm]	β_z [rad]
$\frac{\pi}{32}$	0	0	0.0005	0.001	0.002	$\frac{\pi}{18}$

Field fitting routine

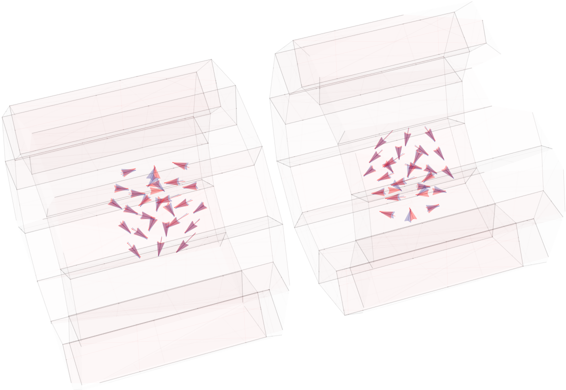

α_x [rad]	α_y [rad]	α_z [rad]	x [mm]	y [mm]	z [mm]	β_z [rad]
$\frac{\pi}{32}$	0	0	0.0005	0.001	0.002	$\frac{\pi}{18}$

Field fitting routine

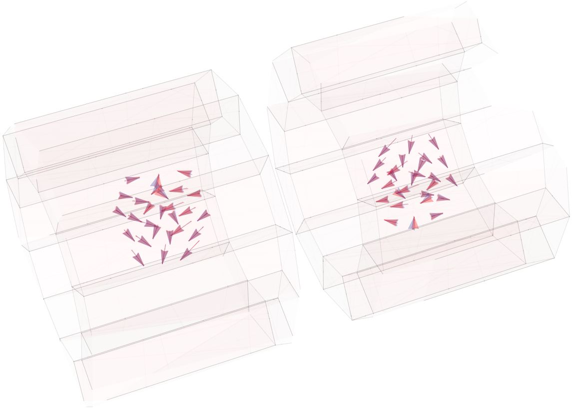

α_x [rad]	α_y [rad]	α_z [rad]	x [mm]	y [mm]	z [mm]	β_z [rad]
$\frac{\pi}{32}$	$\frac{\pi}{64}$	0	0.0005	0.001	0.002	$\frac{\pi}{18}$

Field fitting routine

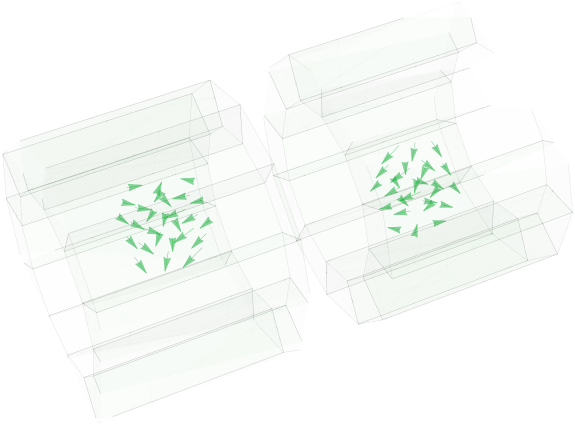

α_x [rad]	α_y [rad]	α_z [rad]	x [mm]	y [mm]	z [mm]	β_z [rad]
$\frac{\pi}{32}$	$\frac{\pi}{32}$	0	0.0005	0.001	0.002	$\frac{\pi}{18}$

Fitting results

- **Measured Grid:**
  $(50 \times 50 \times 50)\,\mu m^3$

- **Simulated Grid:**
  $(16.7 \times 16.7 \times 12.5)\,\mu m^3$

Fitting results

- **Measured Grid:**
  $(50 \times 50 \times 50)\,\mu\mathrm{m}^3$
- **Simulated Grid:**
  $(16.7 \times 16.7 \times 12.5)\,\mu\mathrm{m}^3$

	Sol1	**Sol2**	**Ideal**
x [mm]	0.0333	-0.0333	0.0333
y [mm]	-0.0333	0	-0.0167
z [mm]	-0.0375	-0.025	-0.0375
α_x **[rad]**	10^{-4}	0	2×10^{-4}
α_y **[rad]**	0.0033	0.0032	0.0033
α_z **[rad]**	0	$17\,\pi/16$	0
β_z **[rad]**	0.024	0.024	0.031
$\tilde{\chi}^2$	0.439	0.460	0.460

$$\tilde{\chi}^2 = \frac{\chi^2}{N - n - 1} \approx 1$$